Electron capture by highly charged projectiles under channeling conditions

D. H. Jakubaßa-Amundsen
Physics Section, University of Munich, 85748 Garching, Germany
(Received 9 November 2001; published 24 April 2002)

The impulse approximation for charge transfer in fast, asymmetric ion-atom collisions is modified according to the presence of the axial potential and the geometric target structure when the projectile is axially channeled in a Si single crystal. Calculations of the impact-parameter-dependent capture probability by 1.6–5.6 MeV/amu O^{8+} and S^{16+} show that electron transfer only takes place at short distances to a string of target atoms, combined with a strong reduction as compared to atomic charge transfer.

DOI: 10.1103/PhysRevB.65.174110 PACS number(s): 34.70.+e, 61.85.+p

I. INTRODUCTION

Recent experiments on channeling and dechanneling (also termed ''cooling'' and ''heating'' with respect to the transverse motion) of wide-angle randomly incident ions in single crystals[1,2] have prompted an interpretation in terms of an interplay between electron capture and loss by the projectile when traversing the crystal.[1,3] More precisely, the impact-parameter dependence of the capture-to-loss ratio is assumed to be responsible for the observed effect.

However, little is known about the impact-parameter dependence of electron capture in a single crystal under channeling conditions. There exist calculations on radiative electron transfer where the resulting photon distributions are directly accessible to experiment,[4–6] and on electron capture to continuum by channeled particles where the forward electron yield has been measured.[7] The models used are the impulse approximation[5,6] (for radiative transfer only) or the first Born approximation,[4,7] and the modifications introduced into the theories formulated for ion-single-atom collisions (hereafter denoted by ''atomic'' theories) concern solid-state effects in the target electron momentum distribution as well as consideration of the projectile flux distribution in the crystal channel.

In the case of (nonradiative) electron capture to be discussed below the inclusion of channeling effects is more complicated. An ''atomic'' theory, appropriate for electron transfer in fast, asymmetric ion-atom encounters is the strong potential Born (SPB) theory[8–10] and its on-shell version, the impulse approximation (IA).[9,11] In contrast to the above-mentioned models (where the transition operator is either the radiation field or the electron-projectile interaction) SPB and IA are second-Born-type prescriptions where after being released from the target, the electron propagates in the stronger of the two atomic potentials before it is captured by the projectile. For the fast, heavy projectiles considered below the crystal field is subordinate to the projectile field and therefore enters as transition operator (and not by means of an eigenstate). The adjustment of an ''atomic'' capture theory to channeling conditions involves therefore a modification of the transition operator itself.

In this work a quantum-mechanical calculation of the impact-parameter dependence of electron capture by channeled projectiles is provided. As an underlying ''atomic'' theory, the impulse approximation is used and the crystal field which replaces the atomic potential is treated in the continuum approximation, valid for fast projectiles.[12,13]

The paper is organized as follows. In Sec. II the impulse approximation is briefly described and in Sec. III the interaction potentials and their Fourier transforms are derived. Section IV gives details concerning the evaluation of the capture probability and in Sec. V, results are shown for the impact-parameter-dependent electron capture into the K and L subshells of 25.6, 55, and 89.9 MeV O^{8+} and 110 and 179.8 MeV S^{16+} projectiles. The conclusion is drawn in Sec. VI. Atomic units ($\hbar=m=e=1$) are used unless otherwise indicated.

II. IMPULSE APPROXIMATION

In the semiclassical picture adopted here, the projectile moves along a classical straight-line trajectory characterized by an impact parameter $\mathbf{b}_0$ and the collision velocity $\mathbf{v}$. The dynamics of the active target electron is treated quantum mechanically, and the passive target electrons are accounted for by means of effective potentials. For the sake of simplicity, we shall assume a completely stripped projectile. The post form, to be considered below, of the strong potential Born approximation is valid for heavy projectiles and either light targets or fast collisions (where ''heavy'' and ''light'' mean high and low nuclear charge, respectively). It is derived from the exact amplitude a_{fi} for the transition from a bound electronic target state ψ_i^T to a bound projectile state ψ_f^P which is formally given by the time integral $a_{fi}=-i\int_{-\infty}^{\infty}dt\langle\psi_f^P|V_T|\psi_i^{(+)}\rangle$ (see, e.g., Refs. 9 and 14). $\psi_i^{(+)}$ is an exact solution to the three-body scattering problem, defined by the Lippmann-Schwinger equation $\psi_i^{(+)}=\psi_i^T+GV_P\psi_i^T$, and the potentials V_P and V_T describe the interaction of the electron with the projectile and target, respectively. The approximation concerns the replacement of the full propagator G (in the field V_P+V_T) by the propagator $G_P=(i\partial_t-T_e-V_P+i\epsilon)^{-1}$ in the projectile field alone (where T_e is the kinetic energy of the electron and $\epsilon\to+0$),

$$a_{fi}^{\mathrm{SPB}} = -i\int_{-\infty}^{\infty}dt\langle\psi_f^P|V_T+V_TG_PV_P|\psi_i^T\rangle. \quad (2.1)$$

Introducing a complete set of plane waves $|\mathbf{q}\rangle$, going on-shell and using the definition $(1+G_PV_P)|\mathbf{q}\rangle=|\psi_{\mathbf{q}}^P\rangle$ of a pro-

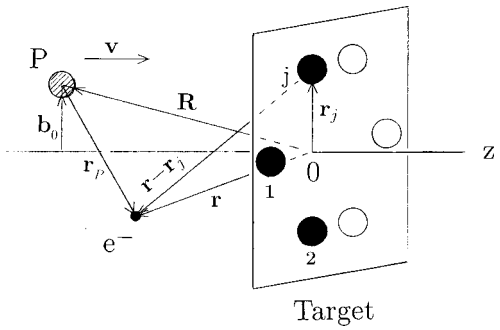

FIG. 1. Schematic collision geometry for a projectile P colliding with a Si target parallel to the $\langle 110\rangle$ axis z. e^- denotes an electron released from atom j of the target. Atoms displayed by filled symbols lie in the plane $z=0$ while empty symbols are projections (along z) of atoms lying in the parallel plane $z=r_j$ where $r_j=3.63$ a.u. is half the channel diameter. The distance of atom 1 from 2 and j is the nearest-neighbor spacing (4.44 a.u.).

jectile scattering eigenstate with momentum $\mathbf{q}$, one arrives at the impulse approximation in its post form,

$$a_{fi}^{\mathrm{IA}}=-i\int_{-\infty}^{\infty}dt\int d\mathbf{q}\langle\psi_f^P|V_T|\psi_{\mathbf{q}}^P\rangle\langle\mathbf{q}|\psi_i^T\rangle. \tag{2.2}$$

From this equation the physics behind the impulse approximation becomes clear: In its post form, the capture amplitude is calculated from the time-reversed process where a projectile electron is excited into a projectile continuum eigenstate which has a strong overlap in momentum space with the state describing a bound target electron in the projectile frame of reference.

Before Eq. (2.2) is evaluated further, the geometry pertaining to a single-crystal target must be specified. A Si crystal has a diamond structure with lattice constant $d=5.43$ Å$=10.25$ a.u.[15] According to Fig. 1, the z axis is chosen parallel to the $\langle 110\rangle$ axial channel which has a configuration of six neighboring atoms.[16] These six-atom layers form a sequence along the z axis, spaced by d. The origin is located at the intersection of the $\langle 110\rangle$ axis with one particular plane that contains three atoms of the channel boundary (1, 2, and j in Fig. 1) while the other three atoms are not situated at $z=0$ but in a parallel plane spaced by half the channel diameter. We denote the positions of the atoms $j=1,\ldots,6$ by $\mathbf{r}_j=(\mathbf{r}_{j\perp},z_j)$ in cylindrical coordinates.

To be specific, assume that atom j provides the electron to be captured. When evaluating the transition amplitude it is convenient to choose the rest system of the heavy projectile as a frame of reference. This means that the initial-state wave function $\psi_i^T(\mathbf{r}-\mathbf{r}_j)$, which originally is defined in the target reference frame, has to be Galilean transformed to the projectile frame of reference. Denoting this transformation by $\hat{U}$ one has[9,10]

$$\hat{U}\psi_i^T(\mathbf{r}-\mathbf{r}_j)e^{-iE_it}=e^{-iv^2t/2}e^{-i\mathbf{v}\mathbf{r}_P}\psi_i^T(\mathbf{r}_P+\mathbf{R}-\mathbf{r}_j)e^{-iE_it}, \tag{2.3}$$

where $\mathbf{R}=\mathbf{b}_0+\mathbf{v}t$ is the coordinate of the projectile, $\mathbf{r}_P$ the electron coordinate in the projectile frame of reference, and E_i the initial-state energy. Forming the overlap of Eq. (2.3) with the plane-wave state $|\mathbf{q}\rangle=(2\pi)^{-3/2}\exp(i\mathbf{q}\mathbf{r}_P)$ and introducing the Fourier representation $\tilde{V}_T(\mathbf{s})$ of the target field $V_T(\mathbf{r})$, the transition amplitude (2.2) takes the form

$$\begin{aligned}a_{fi}^{\mathrm{IA}}(j)=&-i\int_{-\infty}^{\infty}dt\int d\mathbf{q}\frac{1}{(2\pi)^{3/2}}\int d\mathbf{s}\tilde{V}_T(\mathbf{s})\\&\times\langle\psi_f^P(\mathbf{r}_P)|e^{i\mathbf{s}(\mathbf{r}_P+\mathbf{R})}|\psi_{\mathbf{q}}^P(\mathbf{r}_P)\rangle\cdot\frac{1}{(2\pi)^{3/2}}\\&\times\langle e^{i\mathbf{q}\mathbf{r}_P}|e^{-iv^2t/2}e^{-i\mathbf{v}\mathbf{r}_P}\psi_i^T(\mathbf{r}_P+\mathbf{R}-\mathbf{r}_j)\rangle e^{i(\epsilon_f-E_i)t},\end{aligned} \tag{2.4}$$

where ϵ_f is the energy of the final bound state. With

$$\begin{aligned}&\langle e^{i\mathbf{q}\mathbf{r}_P}|e^{-i\mathbf{v}\mathbf{r}_P}\psi_i^T(\mathbf{r}_P+\mathbf{R}-\mathbf{r}_j)\rangle\\&\quad=\int d\varrho\, e^{-i(\mathbf{q}+\mathbf{v})(\mathbf{r}''-\mathbf{R}+\mathbf{r}_j)}\psi_i^T(\varrho)\\&\quad=(2\pi)^{3/2}e^{i(\mathbf{q}+\mathbf{v})\mathbf{R}}e^{-i\mathbf{q}\mathbf{r}_j}\varphi_i^T(\mathbf{q}+\mathbf{v}),\end{aligned} \tag{2.5}$$

where the momentum-space representation φ_i^T of the initial state has been introduced, the time integral becomes trivial and leads to the energy-conserving delta function. Substituting $\mathbf{q}$ by $\mathbf{q}'=\mathbf{q}+\mathbf{s}$ one arrives at the final form,

$$\begin{aligned}a_{fi}^{\mathrm{IA}}(j)=&-\frac{i}{\sqrt{2\pi}}\int d\mathbf{q}'\,\delta\left(\epsilon_f-E_i+\mathbf{q}'\mathbf{v}+\frac{v^2}{2}\right)\\&\times e^{i\mathbf{q}'\mathbf{b}_0}\int d\mathbf{s}\tilde{V}_T(\mathbf{s})M^P(\mathbf{s},\mathbf{q}'-\mathbf{s})\\&\times e^{-i(\mathbf{q}'-\mathbf{s})\mathbf{r}_j}\varphi_i^T(\mathbf{q}'-\mathbf{s}+\mathbf{v}),\\M^P(\mathbf{s},\mathbf{q})=&\langle\psi_f^P(\mathbf{r}_P)|e^{i\mathbf{s}\mathbf{r}_P}|\psi_{\mathbf{q}}^P(\mathbf{r}_P)\rangle.\end{aligned} \tag{2.6}$$

III. INTERACTION POTENTIALS

Let us first calculate the target field induced by the single layer shown in Fig. 1. The potential seen by an electron released from the core state i of atom j has the following structure:

$$\begin{aligned}V(\mathbf{r})=&\sum_{j'=1}^{6}V_N(\mathbf{r}-\mathbf{r}_j')+V_{ci}(\mathbf{r}-\mathbf{r}_j)\\&+\sum_{\substack{j'=1\\j'\neq j}}^{6}V_c(\mathbf{r}-\mathbf{r}_{j'})+V_{\mathrm{val}}(\mathbf{r}),\end{aligned} \tag{3.1}$$

where V_N is the potential of a Si nucleus, V_c the potential of the core electrons, V_{ci} the core potential with electron i removed, and V_{val} the potential of the electron gas originating from the Si valence electrons. We now have to account for the fact that the target consists of a sequence of such layers.

As viewed from the rest system of the projectile, these layers move past the projectile with the velocity $-\mathbf{v}$ at a frequency v/d. In the limit $v/d\to\infty$ the z dependence of the potential disappears and the effective field seen by the released electron is an average over $V(\mathbf{r})$,

$$V_T(\mathbf{r}_\perp)=\frac{1}{d}\int_{-d/2}^{d/2}V(\mathbf{r})dz. \tag{3.2}$$

This defines the axial potential in the continuum approximation.[13] Since d is fixed, the collision velocity must be sufficiently high for this continuum approximation to be valid. The validity criterion given by Lindhard[12] is related to the critical angle $\psi_1=(2Z_PZ_T/Ed)^{1/2}$ for axial channeling, Z_P and Z_T being the nuclear charges of projectile and target atoms, respectively. Let the Thomas-Fermi screening constant $a=0.885(Z_P^{2/3}+Z_T^{2/3})^{-1/2}$ be a measure of the atomic interaction region. If the center-of-mass collision energy E is so large that $\psi_1<a/d$, then a well-channeled particle (and hence also an electron attached to it) traverses the interaction region of many atoms of the $\langle 110\rangle$ string before it is sufficiently deflected to leave the channel. This is a necessary condition for the averaging of $V(\mathbf{r})$ along the projectile path to be meaningful. For a Si target and the projectiles under consideration, the energy required must exceed $E=2$ MeV, which is well satisfied for the present collision systems.

In the formalism of Sec. II, the Fourier transform of $V_T(\mathbf{r}_\perp)$ is needed,

$$\tilde{V}_T(\mathbf{s})=\frac{1}{(2\pi)^{3/2}}\int d\mathbf{r}e^{-i\mathbf{sr}}\frac{1}{d}\int_{-d/2}^{d/2}V(\mathbf{r}_\perp,\lambda)d\lambda. \tag{3.3}$$

Since the interatomic spacing d is much larger than the range of the atomic potential, the integration limits $\pm d/2$ can be replaced by $\pm\infty$.

A. Core potential

The potential V_c originating from the core electrons of a fixed atom j can be expressed in terms of the electron density $\Sigma_{n'}|\psi_{n'}^T(\mathbf{r}'-\mathbf{r}_j)|^2$ where n' runs over the core states (Si K,L subshells) described by the wave functions $\psi_{n'}^T$. The potential seen by a point charge $-e$ at location $\mathbf{r}$ is given by

$$V_c(\mathbf{r}-\mathbf{r}_j)=e^2\sum_{n'}\int d\mathbf{r}'\frac{1}{|\mathbf{r}-\mathbf{r}'|}|\psi_{n'}^T(\mathbf{r}'-\mathbf{r}_j)|^2. \tag{3.4}$$

From Eq. (3.3), the Fourier transform of the averaged core potential is obtained by means of the substitution $\mathbf{x}''_\perp=\mathbf{r}_\perp-\mathbf{r}'_\perp$ for $\mathbf{r}_\perp$,

$$\tilde{V}_c(\mathbf{s};\mathbf{r}_j)=\frac{e^2}{d}\frac{1}{(2\pi)^{3/2}}\int_{-\infty}^{\infty}d\lambda\sum_{n'}\int d\mathbf{x}''_\perp dz\int d\mathbf{r}'_\perp dz'\times\frac{e^{-i\mathbf{s}_\perp(\mathbf{x}''_\perp+\mathbf{r}'_\perp)}e^{-is_zz}}{[x''^2_\perp+(\lambda-z')^2]^{1/2}}|\psi_{n'}^T(\mathbf{r}'-\mathbf{r}_j)|^2. \tag{3.5}$$

Next we replace λ by $\lambda'=\lambda-z'$ and then $\mathbf{r}'$ by $\mathbf{r}''=\mathbf{r}'-\mathbf{r}_j$ such that $\tilde{V}_c$ factorizes into three parts,

$$\tilde{V}_c(\mathbf{s};\mathbf{r}_j)=\frac{e^2}{d(2\pi)^{3/2}}e^{-i\mathbf{s}_\perp\mathbf{r}_{j\perp}}\left(\sum_{n'}\int d\mathbf{r}''e^{-i\mathbf{s}_\perp\mathbf{r}''_\perp}|\psi_{n'}^T(\mathbf{r}'')|^2\right)\cdot\left(\int dze^{-is_zz}\right)\cdot\left(\int_{-\infty}^{\infty}d\lambda'\int d\mathbf{x}''_\perp e^{-i\mathbf{s}_\perp\mathbf{x}''_\perp}\frac{1}{(x''^2_\perp+\lambda'^2)^{1/2}}\right). \tag{3.6}$$

Note that the Fourier transform of the potential is independent of the z component of $\mathbf{r}_j$. The z integral in Eq. (3.6) gives $2\pi\delta(s_z)$ which implies $s_z=0$ everywhere. The last integral is also easily evaluated by introducing the new variable $\mathbf{x}=(\mathbf{x}''_\perp,\lambda')$,

$$\int d\lambda' d\mathbf{x}''_\perp\frac{e^{-i\mathbf{s}_\perp\mathbf{x}''_\perp-is_z\lambda'}}{(x''^2_\perp+\lambda'^2)^{1/2}}=\int d\mathbf{x}e^{-i\mathbf{sx}}\frac{1}{x}=\frac{4\pi}{s^2}=\frac{4\pi}{s_\perp^2}. \tag{3.7}$$

For the remaining integral use is made of the fact that for occupied core states, the electron density is spherically symmetric. With the decomposition $\psi_{n'}^T(\mathbf{r})=R_{nl}(r)Y_{lm}(\hat{\mathbf{r}})$ where the angular part is described in terms of spherical harmonics Y_{lm} with $\hat{\mathbf{r}}$ denoting the angular components of $\mathbf{r}$, one finds in the case of Si (including the spin degrees of freedom),

$$\sum_{n'}|\psi_{n'}^T(\mathbf{r}'')|^2\equiv\frac{1}{4\pi}\tilde{R}(r'')=\frac{1}{2\pi}[|R_{1s}(r'')|^2+|R_{2s}(r'')|^2+3|R_{2p}(r'')|^2], \tag{3.8}$$

where R_{1s},R_{2s}, and R_{2p} are the radial parts of the $1s$,$2s$, and $2p$ wave functions, respectively. Using spherical coordinates $(r'',\vartheta'',\varphi'')$ for $\mathbf{r}''$ the integral can be written in terms of a Bessel transform,

$$\sum_{n'} \int d\mathbf{r}'' e^{-i\mathbf{s}\mathbf{r}''} |\psi_{n'}^{T}(\mathbf{r}'')|^2$$

$$= 2\pi \int_0^\infty r''^2 dr'' \int_{-1}^{1} d(\cos\vartheta'') e^{-isr''\cos\vartheta''} \frac{1}{4\pi} \tilde{R}(r'')$$

$$= \int_0^\infty r''^2 dr'' j_0(sr'') \tilde{R}(r'') \equiv \tilde{R}_0(s), \tag{3.9}$$

where $j_0(x) = \sin x/x$. Recalling that $s_z = 0$ (such that $s = s_\perp$), Eq. (3.6) turns into

$$\tilde{V}_c(\mathbf{s};\mathbf{r}_j) = \frac{e^2}{d} 2\sqrt{2\pi} \frac{1}{s_\perp^2} \delta(s_z) \tilde{R}_0(s_\perp) e^{-i\mathbf{s}_\perp \mathbf{r}_{j\perp}}. \tag{3.10}$$

B. Nuclear potential

The nuclear potential V_N is Coulombic,

$$V_N(\mathbf{r}-\mathbf{r}_j) = -Z_T e^2 \frac{1}{|\mathbf{r}-\mathbf{r}_j|}. \tag{3.11}$$

The Fourier-transformed average potential $\tilde{V}_N(\mathbf{s};\mathbf{r}_j)$ is readily obtained within the above formalism if in Eq. (3.4) and hence in Eq. (3.9) the formal replacement $\Sigma_{n'} |\psi_{n'}^{T}(\mathbf{r}'')|^2 \mapsto -Z_T \delta(\mathbf{r}'')$ is made. Repeating the steps leading to Eq. (3.10) results in

$$\tilde{V}_N(\mathbf{s};\mathbf{r}_j) = -\frac{Z_T e^2}{d} 2\sqrt{2\pi} \frac{1}{s_\perp^2} \delta(s_z) e^{-i\mathbf{s}_\perp \mathbf{r}_{j\perp}}. \tag{3.12}$$

C. Valence potential

When the Si atoms combine to a crystal the valence electrons are released and move freely in the potential of the ionic cores. Hence, the density distribution of the valence electrons has the periodicity of the crystal. For the diamond structure of Si, the valence potential may be approximated by a sum over reciprocal lattice vectors $\mathbf{G}$,[15] which is symmetric in $\boldsymbol{\tau}$ where $\tau = d\sqrt{3}/4$ is the spacing of the closest Si atoms in the unit cell,[17]

$$V_{\rm val}(\mathbf{r}) = \sum_{|\mathbf{G}| \leqslant G_0} \cos(\mathbf{G}\boldsymbol{\tau}/2) V_G e^{-i\mathbf{G}\mathbf{r}} \tag{3.13}$$

with $G_0 = \sqrt{11} \cdot 2\pi/d$ and V_G the form factor corresponding to $\mathbf{G}$. The contribution to the Fourier-transformed averaged potential for a fixed $\mathbf{G}$ follows from

$$\tilde{V}_{\rm val}(\mathbf{s};\mathbf{G}) = \frac{1}{(2\pi)^{3/2}} \int d\mathbf{r} e^{-i\mathbf{s}\mathbf{r}} \frac{1}{d} \int_{-d/2}^{d/2} d\lambda \times \cos(\mathbf{G}\boldsymbol{\tau}/2) V_G e^{-i\mathbf{G}_\perp \mathbf{r}_\perp} e^{-iG_z\lambda}, \tag{3.14}$$

which factors into three integrals,

$$\left(\int d\mathbf{r}_\perp e^{-i(\mathbf{s}_\perp + \mathbf{G}_\perp)\mathbf{r}_\perp} \right) \cdot \left(\int dz e^{-is_z z} \right) \left(\int_{-d/2}^{d/2} e^{-iG_z\lambda} d\lambda \right)$$

$$= (2\pi)^2 \delta(\mathbf{s}_\perp + \mathbf{G}_\perp) \cdot 2\pi\delta(s_z) \cdot \frac{2}{G_z} \sin\frac{G_z d}{2} \tag{3.15}$$

such that one obtains

$$\tilde{V}_{\rm val}(\mathbf{s}) = \sum_{|\mathbf{G}| \leqslant G_0} (2\pi)^{3/2} \frac{2}{dG_z} \cos(\mathbf{G}\boldsymbol{\tau}/2) \times V_G \delta(\mathbf{s}_\perp + \mathbf{G}_\perp) \delta(s_z) \sin\frac{G_z d}{2}. \tag{3.16}$$

Collecting results, the total target potential entering into Eq. (2.6) is given by

$$\tilde{V}_T(\mathbf{s}) = \sum_{j'=1}^{6} \tilde{V}_N(\mathbf{s};\mathbf{r}_{j'}) + \tilde{V}_{ci}(\mathbf{s};\mathbf{r}_j) + \sum_{\substack{j'=1 \\ j' \neq j}}^{6} \tilde{V}_c(\mathbf{s};\mathbf{r}_{j'}) + \tilde{V}_{\rm val}(\mathbf{s})$$

$$\equiv \tilde{V}_T(\mathbf{s}_\perp) \delta(s_z), \tag{3.17}$$

where the individual potentials are defined in Eqs. (3.12), (3.10), and (3.16), while $\tilde{V}_{ci}(\mathbf{s};\mathbf{r}_j)$ is taken from an Eq.-(3.10)-type expression where in $\tilde{R}(r'')$, defined by Eq. (3.8) and entering via Eq. (3.9), the bound-state wavefunction of electron i is omitted. (In case of a p state we assume an average over the magnetic quantum numbers such that the density of the remaining core electrons is still spherically symmetric.)

IV. CAPTURE PROBABILITY AND DETAILS OF CALCULATION

The total capture probability of an electron initially occupying Si core state i into a given subshell f of the projectile is calculated from

$$P_{fi}(\mathbf{b}_0) = 2 \sum_{j=1}^{6} |a_{fi}^{\rm IA}(j)|^2, \tag{4.1}$$

where the sum runs over all six atoms of the target layer (Fig. 1) with $a_{fi}^{\rm IA}(j)$ from Eq. (2.6). The prefactor 2 accounts for the spin degeneracy of the initial subshell.

We now turn to details of the wave functions involved. For a bare projectile the eigenstates ψ_f^P and $\psi_{\mathbf{q}}^P$ are Coulomb functions and the matrix element M^P in Eq. (2.6) is known analytically. For capture into a $1s$ state one has

$$M_{1s}^P(\mathbf{s},\mathbf{q}) = \frac{1}{(2\pi)^{3/2}} \int d\mathbf{r} e^{\pi\eta_q/2} \Gamma(1-i\eta_q) \times e^{i\mathbf{q}\mathbf{r}} {}_1F_1(i\eta_q, 1, i(qr-\mathbf{q}\mathbf{r})) e^{i\mathbf{s}\mathbf{r}} \frac{Z_P^{3/2}}{\sqrt{\pi}} e^{-Z_P r}$$

$$= \frac{4\sqrt{2}}{\pi} Z_P^{5/2} e^{\pi\eta_q/2} \Gamma(1-i\eta_q) [s^2 - (q+iZ_P)^2]^{-i\eta_q - 1} \times [Z_P^2 + (\mathbf{s}+\mathbf{q})^2]^{i\eta_q - 2} \cdot [s^2 + (1+i\eta_q)\mathbf{q}\mathbf{s}], \tag{4.2}$$

where ${}_1F_1$ is a confluent hypergeometric function, Γ the gamma function, and $\eta_q = Z_P/q$ the Sommerfeld parameter. Explicit expressions for the L-subshell capture matrix elements can be found in Ref. 18.

For the target, using spherical coordinates, the Fourier transform of a bound-state wave function can be expressed by means of the Bessel transform

$$\varphi_i^T(\mathbf{q}) = \frac{1}{(2\pi)^{3/2}} \int_0^\infty r^2 dr R_{nl}(r) \int d\Omega e^{-iqr\cos\vartheta} Y_{lm}(\hat{\mathbf{r}}) = \sqrt{\frac{2}{\pi}} (-i)^l Y_{lm}(\hat{\mathbf{q}}) \int_0^\infty r^2 dr j_l(qr) R_{nl}(r), \tag{4.3}$$

where use has been made of the partial-wave decomposition of $\exp(-iqr\cos\vartheta)$. In Eq. (4.3), ϑ denotes the angle between $\mathbf{q}$ and $\mathbf{r}$, and j_l is a spherical Bessel function.

As concerns the target core states, Slater-screened hydrogenic wave functions are used for the innermost shell which allows for an analytic evaluation of the Bessel transforms entering into Eqs. (3.10) and (4.3),

$$\int_0^\infty r^2 dr j_0(qr) R_{1s}(r) = \frac{4Z^{5/2}}{(Z^2+q^2)^2},$$

$$\int_0^\infty r^2 dr j_0(sr) |R_{1s}(r)|^2 = \frac{16Z^4}{(s^2+4Z^2)^2} \tag{4.4}$$

with $Z = Z_T - 0.3$ the effective target charge. For the L-subshell states of the Si atom, Hartree-Fock wave functions are taken, generated numerically with the Herman and Skillman code.[19] Their Bessel transforms are evaluated with the help of a fast Bessel transform routine.[20] In the actual calculations of the capture amplitude, the Bessel transforms are calculated in advance on a large grid of mesh points. This leaves a fourfold integration over the perpendicular components of $\mathbf{s}$ and $\mathbf{q}'$ [note that the two integrals over the respective z components are trivial because of the delta functions in Eqs. (3.17) and (2.6)]. All integrals are well behaved except for a singularity of the capture matrix element (4.2) when $\eta_q \to \infty$ (i.e., for $q = |\mathbf{q}' - \mathbf{s}| = 0$). Since $s_z = 0$ and $q_z' = -(\epsilon_f - E_i + v^2/2)/v$, the singularity can only occur if the collision system is chosen such that $q_z' = 0$. This (square-root) singularity is integrable but for very small $|q_z'|$, the integrand is rapidly oscillating.

Up to now we have considered the case where the electron originates from a target core state. For the sake of completeness we include the formalism for the capture of valence electrons although this process is of no significance as discussed later. For fast collisions these electrons can be treated as constituents of a free-electron gas ($E_i = 0$) confined to a Fermi sphere in momentum space. The momentum-space wave function of such an electron, normalized to unity, is given by[15]

$$\varphi_{i,\mathrm{val}}^T(\mathbf{q}) = \frac{1}{2}\sqrt{\frac{3}{\pi}} \frac{1}{k_F^{3/2}} \theta(k_F - q), \tag{4.5}$$

where θ is the Heaviside step function and $k_F = [3\pi^2(32/d^3)]^{1/3}$ is the Fermi momentum for a Si crystal. In that case, the potential $\tilde{V}(\mathbf{s})$ is calculated from all core electrons which means that the restriction $j' \neq j$ and the term $\tilde{V}_{ci}$ in Eq. (3.17) are dropped.

V. RESULTS

The importance of electron capture for a given collision system can be extracted from dynamical considerations and momentum balance. In the projectile frame of reference, the target electron has initially the energy $E_i + v^2/2$ and finally the energy ϵ_f; hence a large transition probability is expected when $E_i + v^2/2 \approx \epsilon_f$. According to the energy-conserving delta function in Eq. (2.6) this implies that the momentum transfer is subject to $q_z' = -(\epsilon_f - E_i + v^2/2)/v \approx -v$.

That the condition $q_z' \approx -v$ provides large transition amplitudes follows also from the structure of Eq. (2.6) by means of peaking considerations. For Coulomb-type potentials, $\tilde{V}_T(\mathbf{s})$ is largest for $s \to 0$ [due to the denominator $s_\perp^2$ in Eqs. (3.10) and (3.12)], and—for spherically symmetric states—the momentum-space wave function φ_i^T is peaked at zero momentum. This requires $0 \approx \mathbf{q}' - \mathbf{s} + \mathbf{v} \approx \mathbf{q}' + \mathbf{v}$ and hence $q_z' \approx -v$ for the capture amplitude to have a maximum value.

For the collision system selected by experiment,[21] 55 MeV $O^{8+} \to Si$ ($v = 11.73$ a.u.) the matching condition is violated (e.g., for $2p \to L$ transitions with $\epsilon_f = -8$ and $E_i = -3.64$ one gets $q_z' = -5.5$). This means that a considerable momentum has to be supplied both by the initial-state wave function ($\mathbf{q}' - \mathbf{s} + \mathbf{v} \neq 0$) and by the interaction field ($s \neq 0$). This is readily possible for the inner-shell wavefunctions and for Coulombic potentials due to their slow decrease in momentum space. However, the valence potential $\tilde{V}_{\mathrm{val}}$ only provides momenta of the order of a reciprocal lattice vector ($\mathbf{s}_\perp = -\mathbf{G}_\perp$) and therefore can be neglected. On the other hand, the cutoff wave function (4.5) for the valence electrons poses the restriction $|\mathbf{q}' - \mathbf{s} + \mathbf{v}| \leqslant k_F$ which implies $q_z' + v = (-\epsilon_f + v^2/2)/v \leqslant k_F$. Since $k_F = 0.96$ a.u. $< v/2$ and $-\epsilon_f = Z_P^2/2n^2 > 0$, this condition cannot be satisfied for the collision systems under consideration. Even the replacement of the cutoff function by a more realistic Fermi distribution with an exponential tail[15] only provides an insignificant contribution of the valence electrons to the total capture probability.

The dependence on impact parameter is governed by the phase factor $\exp[-i\mathbf{q}'(\mathbf{r}_{j\perp} - \mathbf{b}_0)]$ in Eq. (2.6). Let us define $b = |\mathbf{r}_{j\perp} - \mathbf{b}_0|$ as the distance of closest approach between projectile and target atom j (see Fig. 1), the conventional definition of the impact parameter in ion-atom collisions, and let us for the moment disregard capture from the other five atoms. Due to its oscillatory behavior, the factor $\exp(-iq_\perp' b)$ leads to a significant reduction of any contribution

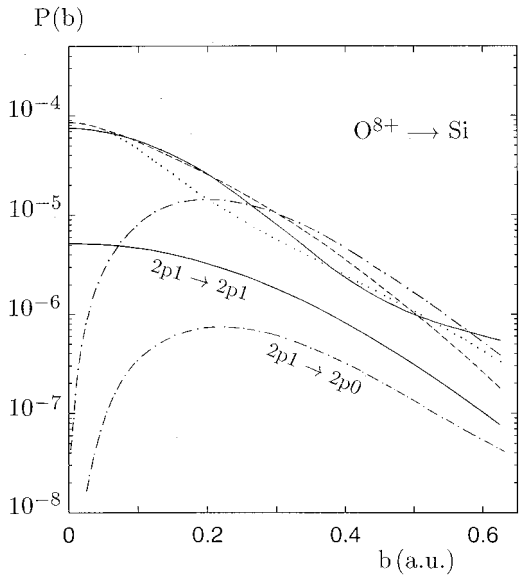

FIG. 2. Capture probability per target electron for 55 MeV O^{8+} ($v=11.73$) traversing a Si single crystal along the $\langle 110\rangle$ direction. Shown are the impact-parameter-dependent capture probabilities from the $2p,m=0$ state of atom j (upper curves) into the projectile K shell (dotted line) and into the $2s$ (dashed line), the $2p,m=0$ (full line), and the $2p,m=1$ (dot-dashed line) subshells. The two lower curves denote the capture probability from the $2p,m=1$ state of atom j into the projectile $2p,m=0$ (dot-dashed line) and $2p,m=1$ (full line) subshells.

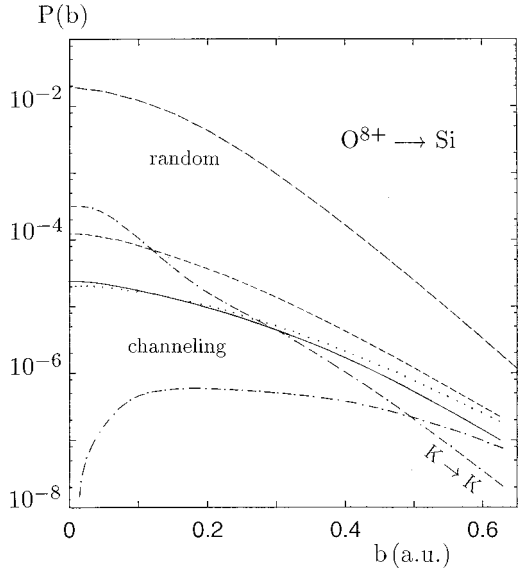

FIG. 3. Capture probability per target electron from the $2s$ state of atom j by 55 MeV O^{8+} projectiles traversing a Si single crystal along the $\langle 110\rangle$ direction. Shown is the impact-parameter dependence for capture into the projectile K shell (dashed line), and into the $2s$ (full line), $2p,m=0$ (dotted line), and $2p,m=1$ (dot-dashed line) subshells. Also given is the capture probability from the K shell into the projectile K shell (two-dash–one-dotted line) as well as the "atomic" capture probability from the $2s$ state into the projectile K shell (dashed line).

to the $\mathbf{q}'$ integral which arises from $q'_\perp b \gg 1$ (even if the two vectors in the exponent are not assumed to be parallel). Hence, the inverse, $q'^{-1}_\perp$, is a measure of the decay length of the capture probability $P(b)$. Assuming $q'_\perp$ to be of the same order of magnitude as the minimum momentum transfer $|q'_z|$, and using that $q'_z \approx -5.5$ for $L \rightarrow L$ transitions, this prescription asserts a width of the impact-parameter distribution of the order of 0.2 a.u.

Figure 2 shows $P(b)=|a_{fi}^{\mathrm{IA}}(j)|^2$ for an electron initially occupying a $2p$ state of atom j according to Fig. 1. Capture probabilities into the K and all L subshells of O^{8+} are given. The transition probabilities from $2p,m=0$ to K, $2s$ and $2p,m=0$ have all decreased for $b=0.2$ a.u. by a factor of e^{-1} or more with respect to $P(b=0)$, which is consistent with the above picture. Exceptions are the transitions which change the m quantum number ($m=0 \rightarrow m=1$ and $m=1 \rightarrow m=0$) which go to zero as $b \rightarrow 0$ because orthogonality of the angular part of the wave functions inhibits capture if no angular momentum is supplied by the transition operator.

All capture probabilities have in common that at $b=0.6$, they have dropped by nearly two orders of magnitude. This means that in the channel center, spaced by $|r_j|=3.63$ a.u. from atom j, the capture probability is completely negligible. But even if capture from an atom were considered for which the spacing to the nearest neighbor is minimum (4.44 a.u.), the capture probability halfway between these two adjacent atoms would be much less than 10^{-4} of its maximum value. As a consequence, at most one of the six atoms of the layer contributes to electron capture at a given $\mathbf{b}_0$.

This in mind we have tentatively switched off the potential of the other five atoms $j' \neq j$ to estimate their contribution to the total interaction field. We have found that for $b \lesssim 0.2$ where the capture probability is high, the influence of the potential of the other atoms can be neglected ($\lesssim 5\%$) while there is a slight reduction of $P(b)$ ($\lesssim 15\%$ as compared to the one-atom potential) for the larger impact parameters considered.

Figure 3 gives the capture probabilities from an initial $2s$ state of atom j. The b dependence is similar as found for the initial $2p$ states, the capture probabilities amounting to at most 10^{-4}. The highest probability at $b \gtrsim 0.6$ is reached for the $2p,m=0 \rightarrow 2p,m=0$ transition (6×10^{-7} at $b=0.6$). The dominant contribution at $b=0$ comes from the $K \rightarrow K$ transition, showing a steep decrease with b. As discussed below, the impulse approximation may, however, be inaccurate for this transition. If summed over all core electrons of target atom j and over all final states considered (projectile K and L shells) the total capture probability is found to be $P_\Sigma(b=0)=1.6\times10^{-3}$ and $P_\Sigma(b=0.62)=4.7\times10^{-6}$.

We have also compared the capture probabilities under channeling conditions with the "atomic" capture probabilities from the collision of an O^{8+} projectile with an isolated Si atom at the same velocity. The latter case will occur for projectile beams at random incidence and thin targets. The capture amplitude for the random case is calculated from Eq. (2.6) with $\mathbf{r}_j$ set equal to zero and with the Fourier-transformed potential given by

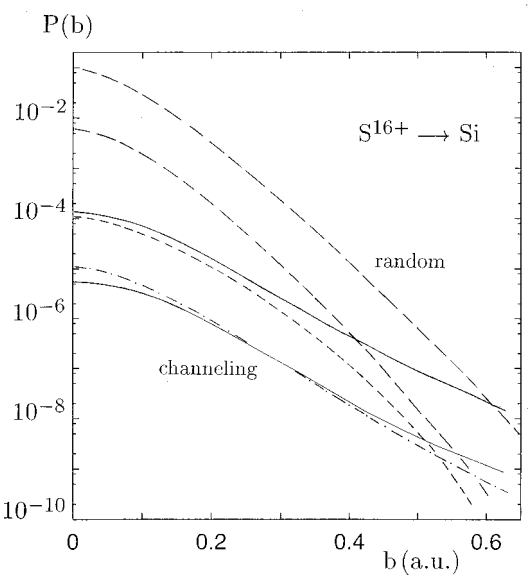

FIG. 4. Capture probability per target electron for S^{16+} projectiles traversing a Si single crystal along the $\langle 110 \rangle$ direction at two different velocities. Shown are the impact-parameter-dependent capture probabilities for $v=15$ (180 MeV) from $K \rightarrow K$ (full, thick line), $K \rightarrow 2s$ (short dashed line), and $2s \rightarrow K$ (full, thin line), and for $v=11.73$ (110 MeV) from $2s \rightarrow K$ (dot-dashed line). Also shown are the ''atomic'' capture probabilities for $v=15$ from $K \rightarrow K$ (long dashed line, upper curve) and from $2s \rightarrow K$ (long dashed line, lower curve).

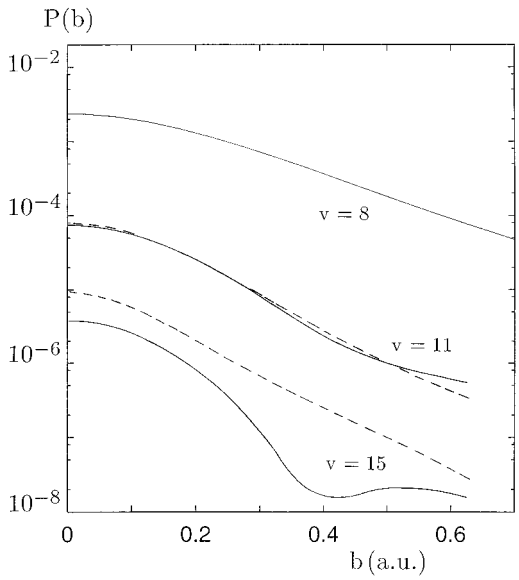

FIG. 5. Capture probability for a $2p,m=0$ Si electron into the $2p,m=0$ shell of an O^{8+} or a S^{16+} projectile at collision velocities $v=8$, 11.73, and 15 during $\langle 110 \rangle$ axial channeling as a function of impact parameter. The full lines are the results for O^{8+}, the dashed lines correspond to S^{32+}.

$$\tilde{V}_{T,\mathrm{ran}}(\mathbf{s}) = e^2 \sqrt{\frac{2}{\pi}} \frac{1}{s^2} \times \left(-Z_T + \tilde{R}_0(s) - \int_0^\infty r^2 dr j_0(sr) |R_i(r)|^2 \right) \tag{5.1}$$

with $\tilde{R}_0(s)$ from Eq. (3.9). The last term corrects for the absence of the electronic state i, initially occupied by the active electron, in the potential. From Fig. 3 it is obvious that for small b, capture under channeling conditions is reduced by as much as two orders of magnitude as compared to capture by randomly incident projectiles, whereas the decrease with impact parameter is much slower in the channeling case. This is related to the fact that the continuum potential is on the one hand much weaker than the atomic potential (the reduction being of the order of $a_0/d \sim 4 \times 10^{-2}$ for Si with $a_0 = 0.885 Z_T^{-1/3}$), but it is, on the other hand, of infinite range in the axial direction because of the averaging [Eq. (3.2)].

Figure 4 shows capture probabilities for the heavier S^{16+} projectiles at two different velocities, $v=11.73$ and $v=15$ (corresponding to beam energies of 3.44 and 5.62 MeV/amu). At the higher velocity, results for the random situation for $K \rightarrow K$ and $2s \rightarrow K$ captures are also included. For this collision system capture under channeling conditions is actually dominant at $b > 0.6$. Capture from the target K shell is about one order-of-magnitude larger than capture from the $2s$ subshell, which also holds for the lower velocity. In contrast, for the lighter O^{8+} projectile, capture from the K shell only dominates at small impact parameters (Fig. 3). The reason is that the momentum $q_z' + v$ which has to be supplied by the initial-state wave function is much higher for S^{16+} than for O^{8+}, favoring capture from the K shell with its wider momentum distribution.

In Fig. 5 the velocity dependence of the $2p,m=0 \rightarrow 2p,m=0$ capture probability is depicted for O^{8+} and S^{16+} projectiles. There is a monotonic decrease of the capture probability with velocity for both projectiles (in contrast to the situation of the $2s \rightarrow K$ capture for S^{16+}, Fig. 4, where $v=11.73$ and $v=15$ lead to similar capture probabilities). For an explanation, one may again consider the deviation of $q_z' + v$ from zero. For the $2p,m=0 \rightarrow 2p,m=0$ transition with O^{8+} projectiles, one has $q_z' + v = 4.5$, 6.24, and 7.8 for $v=8$, 11.73, and 15, respectively, and the numbers for the S^{16+} projectiles are $q_z' + v = 8.3$ and 9.4 for $v=11.73$ and 15, respectively (whereas for S^{16+} and the $2s \rightarrow K$ transition, one gets a slightly smaller value for the higher velocity, $q_z' + v = 16.3$ and 15.7 for $v=11.73$ and 15, respectively).

We close this section with some comments on the approximations inherent in the above theory for electron capture by channeled projectiles. The underlying ''atomic'' theory, the impulse approximation in its post form, is valid for $Z_P/\tilde{n} \gtrsim Z_T/n$ if $v \gg Z_P/\tilde{n}$ or for $Z_P/\tilde{n} \gg Z_T/n$ if $v \gtrsim Z_P/\tilde{n}$ where $\tilde{n}$ and n denote the main quantum numbers of the projectile final state and target initial state, respectively. The first inequality determines the asymmetry of the collision system while the second inequality defines ''fast collision'' in terms of the classical electron orbiting velocity for the heavier of the two collision partners.

For the present collision systems, capture from the target

K shell is the most pathological case. *K*-shell capture by the O^{8+} projectiles does not satisfy the IA validity criterion, whereas it is marginally satisfied by the heavier S^{16+} projectiles. In the channeling case, Z_T/n does not seem to be the appropriate measure of the interaction strength with the target, taking into consideration the strongly reduced potential in the continuum approximation. This would suggest that the IA is applicable for capture from and to all *K*- and *L*-shell states even for O^{8+}, provided $v \gtrsim Z_P/\tilde{n}$. Nevertheless, IA results violating the above-mentioned validity criterion should be treated with some care.

As concerns the description of the target field, the initial state *i* of the active electron is not included in the core potential. However in the channeling situation, the electron will interact with different atoms of the string which do not have an inner-shell vacancy. In order to estimate the importance of an inner-shell vacancy, we have made test calculations with a potential corresponding to fully occupied core states. When compared to previous results, the capture probability is lowered, $<10\%$ for small impact parameters, but as much as 35% for the larger b ($\lesssim 0.6$ a.u.) in the case of capture from the *K* shell. For capture from the L shell which dominates at large b, the reduction is smaller ($\lesssim 10\%$ for $b \lesssim 0.6$ a.u.). This decrease of $P(b)$ when core state *i* is added is due to the reduction of the attractive total core potential $V_N + V_c$ as compared to $V_N + V_{ci}$.

Another approximation which might be questioned is the calculation of the target core states from a neutral-atom code, as well as the use of experimental binding energies for an isolated atom. Inside the solid, the valence electrons are lost which consequently will lead to a modification of the core states. When the outer electrons are removed, i.e., the screening of the central field is weakened, the core-state binding energies will get larger. In turn, this implies some reduction of the capture amplitude. However, this is likely to be compensated by an enlarged spread of the core-state wave functions in momentum space. The additional approximations pertaining to a crystal target, the continuum approximation for the target field, the neglect of the valence electrons, as well as the disregard of multiple capture from different strings are well justified in the present situation.

VI. CONCLUSION

The impulse approximation in its post form, applicable for heavy projectiles and high collision velocities, has been used to calculate electron capture by energetic, fully stripped projectiles channeling through a single crystal. Due to the large momentum transfer required, only capture from the target core states plays any role. Results have been provided for capture into the projectile *K* shell and *L* subshells. For the present collision systems, $K \rightarrow K$ transfer is the most important process at small impact parameters with respect to a string of atoms. At the larger impact parameters, $2p, m=0 \rightarrow 2p, m=0$ subshell capture gives the dominant contribution. We have found that, due to the weakness of the crystal field treated in the continuum approximation, the capture probabilities are very small. For the collision systems investigated, they amount to at most $\sim 10^{-4}$ for a given subshell transition at small impact parameters. This number is about two orders-of-magnitude smaller than that for an isolated ion-atom collision. If summed over the core states of a target atom and over the final *K*-shell and *L*-subshell states of the projectile, the total capture probability $P_\Sigma(b=0)$ is $\sim 10^{-3}$. Inclusion of *M*-shell and higher final states will not change this result because capture to higher states with a narrower momentum distribution is expected to be less important than capture to the innermost shells.

Since large momenta can only be supplied in close collisions, the transition probability decreases rapidly towards the center of the crystal channel. The width of the impact-parameter distribution is, however, considerably larger than the corresponding width in an isolated ion-atom collision, because the range of the continuum potential is infinite along the axial direction. Nevertheless, the capture probabilities have decreased by many orders of magnitude in the channel center such that a folding with the beam profile of well-channeled projectiles will lead to negligible capture probabilities. Even if taken into consideration that our results suffer from many approximations related to the description of solid-state effects and therefore may readily be inaccurate by a factor of 2, this excludes any interplay between electron capture and loss which was postulated to describe the experimental data. Also, the smooth dependence of the capture probabilities and of the width of the impact-parameter distributions, both on collision velocity and projectile charge, does not provide any explanation of the sharp transition[2] in v and Z_P from cooling to heating in single crystals.

Rather, the present results should be considered as a benchmark showing that phenomena well known from ion-atom collisions may basically change inside a solid. In particular, all processes requiring large momentum transfers will be strongly suppressed in the case of well-channeled beams.

ACKNOWLEDGMENTS

I would like to thank W. Assmann for stimulating this project, and F. Grüner and H. Rothard for helpful discussions.

[1] W. Assmann, H. Huber, S.A. Karamian, F. Grüner, H.D. Mieskes, J.U. Andersen, M. Posselt, and B. Schmidt, Phys. Rev. Lett. **83**, 1759 (1999).

[2] F. Grüner, M. Schubert, W. Assmann, F. Bell, S.A. Karamian, and J.U. Andersen, Nucl. Instrum. Methods Phys. Res. B (to be published).

[3] S.A. Karamian, W. Assmann, K. Ertl, D. Frischke, H.D. Mieskes, B. Schmidt, and S.P. Tretyakova, Nucl. Instrum. Methods Phys. Res. B **164**, 61 (2000).

[4] B.R. Appleton, R.H. Ritchie, J.A. Biggerstaff, T.S. Noggle, S. Datz, C.D. Moak, H. Verbeek, and V.N. Neelavathi, Phys. Rev. B **19**, 4347 (1979).

[5] J.E. Miraglia, R. Gayet, and A. Salin, Europhys. Lett. **6**, 397 (1988).
[6] S. Andriamonje, M. Chevallier, C. Cohen, N. Cue, D. Dauvergne, J. Dural, F. Fujimoto, R. Kirsch, A. L'Hoir, J.-C. Poizat, Y. Quéré, J. Remillieux, C. Röhl, H. Rothard, J. P. Rozet, D. Schmaus, M. Toulemonde, and D. Vernhet, Phys. Rev. A **54**, 1404 (1996).
[7] M.N. Khan and M.W. Lucas, Phys. Rev. B **19**, 5578 (1979).
[8] J.H. Macek and R. Shakeshaft, Phys. Rev. A **22**, 1441 (1980).
[9] D.H. Jakubaßa-Amundsen and P.A. Amundsen, Z. Phys. A **297**, 203 (1980).
[10] D.H. Jakubaßa-Amundsen, Int. J. Mod. Phys. A **4**, 769 (1989).
[11] J.S. Briggs, J. Phys. B **10**, 3075 (1977).
[12] J. Lindhard, Mat. Fys. Medd. K. Dan. Vidensk. Selsk. **34**, No. 14, 1 (1965).
[13] P. Lervig, J. Lindhard, and V. Nielsen, Nucl. Phys. A **96**, 481 (1967).
[14] M.R.C. McDowell and J.P. Coleman, *Introduction to the Theory of Ion-Atom Collisions* (North-Holland, Amsterdam, 1970), p. 206; Chap. 6.
[15] C. Kittel, *Einführung in die Festkörperphysik* (Oldenbourg, München, 1969), pp. 48, 255, and 311 [*Introduction to Solid State Physics* (Wiley, New York, 1986), pp. 19, 130, and 167].
[16] A. L'Hoir, S. Andriamonje, R. Anne, N.V. de Castro Faria, M. Chevallier, C. Cohen, J. Dural, M.J. Gaillard, R. Genre, M. Hage-Ali, R. Kirsch, B. Farizon-Mazuy, J. Mory, J. Moulin, J.C. Poizat, Y. Quéré, J. Remillieux, D. Schmaus, and M. Toulemonde, Nucl. Instrum. Methods Phys. Res. B **B48**, 145 (1990).
[17] M.L. Cohen and T.K. Bergstresser, Phys. Rev. **141**, 789 (1966).
[18] D.H. Jakubaßa-Amundsen, Phys. Rev. A **38**, 70 (1988).
[19] F. Herman and S. Skillman, *Atomic Structure Calculations* (Prentice-Hall, Englewood Cliffs, NJ, 1963).
[20] J.D. Talman, Comput. Phys. Commun. **30**, 93 (1983).
[21] F. Grüner, Diploma thesis, University of Munich, 2000.